Ab initio optoelectronic properties of SiGe nanowires: Role of many-body effects

Maurizia Palummo,[1,*] Michele Amato,[2] and Stefano Ossicini[3]
[1]*European Theoretical Spectroscopy Facility (ETSF), CNR-INFM-SMC, Dipartimento di Fisica, Università di Roma, "Tor Vergata," via della Ricerca Scientifica 1, 00133 Roma, Italy*
[2]*"Centro S3," CNR-Istituto di Nanoscienze, Dipartimento di Fisica, Università di Modena e Reggio Emilia, via Campi 213/A, 41100 Modena, Italy*
[3]*European Theoretical Spectroscopy Facility (ETSF), "Centro S3," CNR-Istituto di Nanoscienze, Dipartimento di Scienze e Metodi dell'Ingegneria, and Centro Interdipartimentale "En&Tech," Università di Modena e Reggio Emilia, via Amendola 2 Pad. Morselli, 42100 Reggio Emilia, Italy*

(Received 27 April 2010; revised manuscript received 24 July 2010; published 13 August 2010)

The self-energy and electron-hole interaction corrections to the one-particle approximation for SiGe nanowires have been calculated for different geometries and diameters. We show that, at fixed nanowire diameter and orientation, the self-energy corrections for the SiGe nanowires can be obtained as a weighted average, on the relative composition of one type of atom with respect to the total numbers of atoms in the unit cell, of the corrections for the pure (Si and Ge) nanowires, thus circumventing cumbersome computations and allowing a direct and practical determination of the electronic band gap. Moreover we show that particular geometrical configurations are at the origin of an enhancement of the optical oscillator strength that should be important for optoelectronic applications.

DOI: 10.1103/PhysRevB.82.073305 PACS number(s): 73.22.−f, 73.21.Hb, 71.15.Mb, 78.67.−n

The research activity on semiconducting nanowires (NWs) is one of the most rapidly developing area in material science due the variety of important applications which, in the last years, has been envisaged in the fields of electronics,[1] optoelectronics,[2] nanomedicine,[3] and bioelectronics.[4] Due to their compatibility with the existing Si-based microelectronics, Si,[5] but also Ge and SiGe NWs have been the subject of intense experimental[6–11] and theoretical[12–23] investigations. Regarding SiGe NWs, particular attention has been devoted to *core-shell* NWs due to their good performances as high-mobility FETs,[24] furthermore recent experiments have shown the possibility to tune the NW's band gap (BG) by varying the relative Si and Ge concentrations.[8] By means of *ab initio* investigations we have recently studied the electronic properties of several kind of Si,[16] Ge,[12] and SiGe NWs.[25,26] It has been proved that the measured Si NWs electronic gaps[7] can be well reproduced only when the one-particle density-functional theory (DFT) scheme is overcome and the self-energy (GW) corrections are added to the underestimated local-density approximation (LDA) gaps.[14,16] Moreover a good agreement between calculated and measured optical properties can be found only if also the electron-hole (e-h) interaction is taken into account.[16] Similar results have been obtained for Ge NWs.[12,17] Regarding the SiGe NWs, we have demonstrated how some particular geometries show an intriguing electronic and optoelectronic behavior to be used for solar-cell applications.[25] However a complete *ab initio* study of these nanostructures (NSs), with the inclusion of many-body effects, is still missing. The aim of this work is, thus, twofold: first we show how, starting from the analysis of the results for pure Si and Ge NWs, the computed GW corrections of SiGe NWs can be obtained as a weighted average (on the relative composition x of one type of atom with respect to the total number of atoms in the unit cell) of the GW corrections of the pure (Si and Ge) NWs with the same diameter and crystalline orientation and that, indeed, they are independent from the geometry of the system. We underline that this is an important information because it allows to avoid cumbersome GW calculations for all the possible SiGe NWs. Then we discuss how the SiGe alloying allows to tailor the optical properties from the pure Si to the pure Ge limits and how for particular geometrical atomic configurations it can be at the origin of an enhancement of the optical oscillator strength in the infrared (IR) region. The geometrical structures of the free-standing hydrogenated NWs investigated here are the same considered in Refs. 25 and 26: they are oriented along the [110] direction and have a diameter ranging from 1.1 to 1.9 nm.[27] As regards as SiGe NWs, we have analyzed *mixed* (with $x_{Si}=0.5$), *abrupt* (with $x_{Si}=0.31$, 0.5, 0.69), Si_{core}/Ge_{shell} NWs (with $x_{Si}=0.33$, 0.4, 0.66), and Ge_{core}/Si_{shell} (with $x_{Si}=0.66$) NWs.[28] It is important to point out that the mixed geometry is only a theoretical model which does not reproduce the experimental situation but which is useful in order to investigate how the intermixing between Si and Ge atoms can affect the optical properties with respect to other structures that have a sharp Si/Ge interface.

The present study is carried out using a many-body perturbation-theory approach by means of a well-established theoretical/computational scheme.[29,30] First the ground-state electronic properties of the relaxed NWs are obtained by performing DFT-LDA calculations, using the QUANTUM-ESPRESSO package.[31,32] Then in order to obtain a predictive estimations of the charged electronic excitations, the quasiparticle corrections to the LDA eigenvalues are evaluated within the G_0W_0 approximation for the self-energy operator, where the LDA wave functions are used as good approximations for the quasiparticle ones, and the screening W_0 is treated within the random phase approximation using a plasmon-pole model to describe its energy dependence.[30] While to calculate the NWs optical properties, taking into account their intrinsic excitonic nature, we have solved the

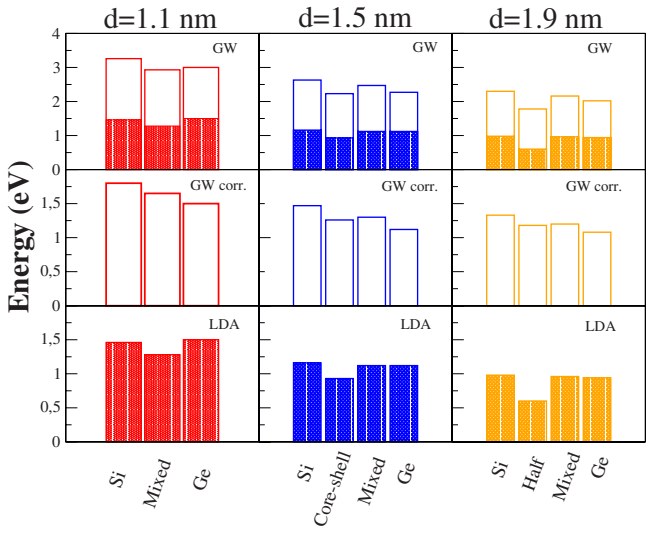

FIG. 1. (Color online) LDA gaps (bottom panels), GW corrections (middle panels), GW gaps (top panels) for Si, Si_xGe_{1-x}, and Ge NWs of $d=1.1$ nm (left), $d=1.5$ nm (central), and $d=1.9$ nm (right). The atomic configurations are specified below the bottom axis. In all the mixed and abrupt NWs considered here $x_{Si}=0.5$. While for the Si_{core}/Ge_{shell} wire is $x_{Si}=0.4$.

Bethe-Salpeter equation (BSE) in the basis set of quasielectron and quasihole states.[30]

In Fig. 1 we show the calculated DFT-LDA (bottom panels), quasiparticle (top panels) electronic gaps together with the corresponding self-energy corrections (central panels) for Si, Ge, and some of the SiGe NWs studied here while a complete report is presented in Table I. We show them from left to right for three different diameters: $d=1.1$, 1.5, and 1.9 nm. At the DFT-LDA level[25,26] (see also the first column of Table I, E_{KS}^{gap}), whereas the mixed NWs present a scaling of the BG with diameter that is very similar to the trend obtained for the pure NWs, in the case of abrupt and core-shell NWs, where a sharp interface is present, the LDA BGs show a reduced quantum confinement effect (RQCE) with respect to the corresponding pure NWs (i.e., for the same diameter the BG is smaller). This effect is present if both the extrinsic (diameter) and intrinsic (relative composition and geometry of Si/Ge interface) parameters of the wire are modulated. The entity of this RQCE depends on the specific geometry of the SiGe NWs: in particular, abrupt NWs present the most pronounced RQCE and a perfect parabolic dependence of the electronic BG on the composition. We have related this behavior to the type II band offset that comes out at the planar interface of Si and Ge.[25,26] From these results we can deduce that, at LDA level, is not possible to infer the values for the BG of the SiGe NWs, directly from those of pure Si and Ge NWs but it is necessary to perform a DFT calculation for every considered geometry. Fortunately the situation is quite different for the quasiparticle corrections. In fact looking at the central panels of Fig. 1 and at the second column of Table I (ΔE_{GW}^{c}), it results that the GW corrections of SiGe NWs, similarly to the ones for pure Si and Ge NWs,[12,14,16] strongly increase reducing the NW diameter and, more importantly, they are smoothly approximated by a weighted average of the two GW corrections calculated for the pure Si and Ge NW with the same diameter as: $\Delta E_{GW}(Si_xGe_{1-x}NW) = x\Delta E_{GW}(SiNW) + (1-x)\Delta E_{GW}(GeNW)$ (reported in the third column of Table I as $\Delta^a E_{GW}$). This conclusion seems to be independent from the atomic configurations (mixed, core shell, or abrupt) and to be mainly dependent from the relative composition of the two atomic species. In the bottom part of Table I we report the GW correction calculated at Γ point for Si, Ge, and $Si_{0.5}Ge_{0.5}$ bulk compounds, using the same pseudopotentials and computational tools. These values seem to give an indication that the rule presented above could be probably applied also in these systems, nevertheless in order to verify this conclusion, more cumbersome GW calculations in extended supercells should be performed and this is clearly beyond the scope of the present Brief Report. Furthermore we think that the main physical origin of the validity of the *composition rule* in NWs can be ascribed to the fact that in such confined and totally immersed in vacuum systems, the screened Coulomb potential $W=\epsilon^{-1}V$, which enters in the calculation of the *GW* corrections, is essentially determined by the dominant role of the vacuum (which surrounds the NW) and by its dielectric function. To strength this idea it is worth to mention that we have observed a weak dependence of the GW correction (at fixed NW size) to very different DFT-LDA electronic gaps, both doping the NW with III and V groups elements[23] and also changing the surface termination.[33] Our calculated quasiparticles electronic gaps of pure Si and Ge NWs have been fitted using an in-

TABLE I. First column: Kohn-Sham DFT-LDA minimum (direct) gaps. The calculated self-energy corrections are reported in the second column and are compared with the corresponding values obtained from the averaged composition rule (third column), as discussed in the text. All the values are in eV and are calculated at Γ point. Mx: mixed. Ab: abrupt. CS: core shell (Si_xGe_{1-x} refers to Si_{core}/Ge_{shell} while Ge_xSi_{1-x} refers to Ge_{core}/Si_{shell}).

		E_{KS}^{gap}	ΔE_{GW}^{c}	ΔE_{GW}^{a}
$d=1.9$	Ge	0.94	1.07	
	Si	0.98	1.34	
	$Si_{0.5}Ge_{0.5}$ (Mx)	0.96	1.20	1.21
	$Si_{0.5}Ge_{0.5}$ (Ab)	0.96	1.19	1.21
	$Si_{0.31}Ge_{0.69}$ (Ab)	0.73	1.15	1.16
	$Si_{0.69}Ge_{0.31}$ (Ab)	0.69	1.22	1.2
	$Si_{0.33}\bar{}Ge_{0.66}\bar{}$ (Cs)	0.71	1.15	1.14
	$Si_{0.66}\bar{}Ge_{0.33}\bar{}$ (Cs)	0.91	1.17	1.25
$d=1.5$	Ge	1.12	1.14	
	Si	1.15	1.46	
	$Si_{0.5}Ge_{0.5}$ (Mx)	1.14	1.31	1.30
	$Ge_{0.4}Si_{0.6}$ (Cs)	1.11	1.34	1.33
	$Si_{0.4}Ge_{0.6}$ (Cs)	0.93	1.28	1.26
$d=1.1$	Ge	1.50	1.51	
	Si	1.46	1.82	
	$Si_{0.5}Ge_{0.5}$ (Mx)	1.28	1.64	1.66
Bulk	Ge	0.24	0.59	
	Si	2.57	0.65	
	$Si_{0.5}Ge_{0.5}$ (Mx)	1.80	0.64	0.62

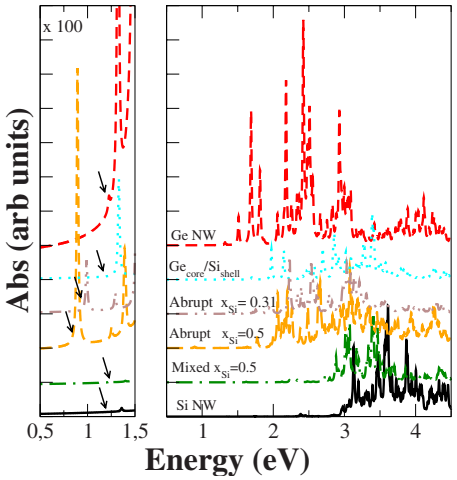

FIG. 2. (Color online) Right panel: BSE spectra of NWs with $d=1.9$ nm. Si (bottom black full curve), Ge (top red/dark gray long-dashed curve), mixed SiGe with $x_{Si}=0.5$ (green dotted-dashed curve), Ge_{core}/Si_{shell} with $x_{Si}=0.67$ (cyan dot curve), abrupt SiGe with $x_{Si}=0.31$ (brown double-dotted-dashed curve), and abrupt SiGe with $x_{Si}=0.5$ (orange/light gray long-dashed curve). Left panel: low-energy part zoom. The arrows indicate the onset of optical spectra.

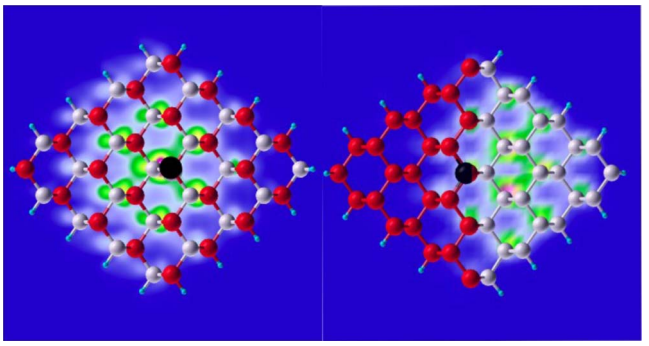

FIG. 3. (Color online) Probability distribution $|\psi_{exc}(r_e,r_h)|^2$ for finding the electron when the hole is fixed in a given position (black dot) for mixed NWs (left panel) and abrupt (right panel) NWs (Ref. 25). Large red/dark gray (Ge), large white (Si), and small light blue/light gray (H) spheres.

verse power law as function of diameter, $E_{NW}^{gap}=E_{bulk}^{gap}+\frac{A}{d^{\alpha}}$, and the following parameters $A=2.5$ and 2.7 and $\alpha=1.2$ and 1.1 have been obtained for Si and Ge NWs, respectively. These α values are smaller than 2, the value predicted by simple particle in a box models and, for Si NWs, are in agreement with previous theoretical works with self-energy corrections included.[14,16] At the same time, fitting in a similar way, the GW corrections separately ($\Delta E_{NW}^{GW}=\Delta E_{bulk}^{GW}+\frac{\beta}{d^{\gamma}}$), we obtain $\beta=1.28$ and 1.01 and $\gamma=1.02$ and 1.30 for Si and Ge NWs, respectively. These fits and the average rule illustrated above, allow to avoid heavy GW calculations for the SiGe NWs and permit an easier estimation of the electronic band gap, useful for experimental purposes.

In the last decades a great effort has been dedicated to obtain light emission from Si-based NSs;[34] moreover number of different ways to engineering and improving efficient light emission in Si NSs have been developed. The main objectives of these approaches are to reach a genuine or perceived compatibility with conventional complementary metal-oxide semiconductor technology and to increase the efficiency of radiative e-h recombination.[35] One of these approaches is based on the use of SiGe nanostructures: in fact despite difficulties with their epitaxial growth, two-dimensional and three-dimensional SiGe NSs have been intensively studied as a solution to confine e-h pairs and to reduce the luminescence thermal quenching.[35] More recently also one-dimensional SiGe NSs have been studied and, as envisaged in Ref. 8, the possibility to tailor the optical gap of SiGe NWs, varying both the composition and the diameter, provides challenging opportunities for Si optoelectronics because it potentially allows emission and detection of the photons in the wavelength range of optical fiber communication. For this reason we aim to discuss here the optical properties (obtained within the *ab initio* BSE approach) of some of the studied SiGe NWs and compare them with the corresponding spectra of pure Si and Ge NWs. In the right panel of Fig. 2 we show the optical-absorption spectra (for light polarized along the wire axis), for pure Si, pure Ge NWs and four different types SiGe NWs (see the caption of Fig. 2). On the left panel, the corresponding low-energy region is zoomed. First of all, we point out the evident redshift moving from pure Si and Ge NWs to abrupt SiGe NWs. Similar theoretical results have been demonstrated for SiGe nanodots and superlattices (with sharp Si/Ge interface)[36,37] and, although the NWs presented here are smaller than the typical experimental sizes, they are qualitative in agreement also with experimental observations[8] about random SiGe NWs. A striking difference between abrupt and mixed NWs (both with $x_{Si}=0.5$) can be noted looking at the central curves of the left panel: while in the mixed NW the onset of the optical spectrum is at 1.24 eV (where the lowest exciton is at 1.36 eV and 1.22 eV for Si and Ge NWs, respectively), in the abrupt NWs, with $x_{Si}=0.5$ and 0.31, a very intense peak is present in the IR region at 0.9 eV and 1 eV, respectively. We can ascribe the main origin of this optical behavior to the different geometry that abrupt and mixed NWs have: the first ones present an abrupt interface between Si and Ge regions which favors a type II band offset (with the valence states (VSs) localized on Ge atoms and the conduction states (CSs) localized on Si atoms). This strongly reduces the electronic BG with respect to the pure wires and is responsible for the redshift of the first excitonic peak.

Mixed NWs instead are a perfect intermixed SiGe alloy, where there is not the condition for the formation of a type II band offset. As a result of intermixing (as already clearly theoretically and experimentally demonstrated for SiGe superlattices[37]) the valence band (VB) changes in the direction of approaching the Si VB (therefore lowering its energy) while the conduction band (CB) changes in the direction of approaching the CB of Ge (therefore increasing its energy): this behavior causes a widening of the electronic BG (which becomes similar to the one of pure NWs) and therefore any substantial redshift has not been found in the theoretical spectra with respect to the pure NWs. Probably the redshift observed by Yang *et al.*[8] for random SiGe NWs can be due to the presence of some sharp Si/Ge interfaces between Si and

Ge islands randomly distributed, which are responsible of a RQCE and of a consequent change in the optical absorption with respect to the pure wires. The optical spectra of core-shell NW does not show an appreciable redshift with respect to the pure wires: the main cause of this difference can be ascribed to the fact that, as we have explained in Ref. 26, for core-shell geometry the analysis of the band-gap scaling with the composition is quite complicated also at LDA level, in particular, Ge_{core}/Si_{shell} NWs show almost no reduction in the band gap. Furthermore due to the small diameters, it is not possible to observe, for core-shell NWs, a strong localization of VS and CS and therefore define a clear type II band offset. In fact in these NWs, Si and Ge states are confined in different ways if they constitute the core or the shell of the wire.[26] The situation is probably different for much larger wires but the related many-body calculations are beyond the present computational limits.

Interestingly the redshift of the first excitonic peak in the abrupt geometry (see left panel of Fig. 3) is associated with an increase in the oscillator strength with respect to those of the pure and mixed cases. Looking at the probability distribution $|\psi_{exc}(r_e, r_h)|^2$ (Fig. 3), associated to the lowest energy exciton, for finding the electron when the hole is fixed in the most probable position,[25] it is clear that in mixed NWs (left panel) there is not a spatial separation of electron and hole, as a consequence of the intermixed geometry that does not create the conditions for a spatial localization of VS and CS while, as already demonstrated,[25] abrupt (right panel) NWs have a straightforward tendency to an e-h separation that make them ideal candidates for photovoltaic applications.

This work is supported by MIUR-PRIN 2007 and by EC through e-I3 ETSF project (INFRA-2007-1.2.2: Grant Agreement No. 211956). We acknowledge SuperComputing Center CINECA for CPU time granted by CNR-INFM.

*maurizia.palummo@roma2.infn.it

[1] Y. Huang *et al.*, Science **294**, 1313 (2001).
[2] C. J. Barrelet *et al.*, Nano Lett. **6**, 11 (2006).
[3] K.-Y. Lee *et al.*, Nanoscale. Res. Lett. **5**, 410 (2010).
[4] F. Patolsky *et al.*, Nat. Protoc. **1**, 1711 (2006).
[5] R. Rurali, Rev. Mod. Phys. **82**, 427 (2010).
[6] L. Lauhon *et al.*, Nature (London) **420**, 57 (2002).
[7] D. D. D. Ma *et al.*, Science **299**, 1874 (2003).
[8] J. Yang *et al.*, Nano Lett. **6**, 2679 (2006).
[9] Y. Hu *et al.*, Nat. Nanotechnol. **2**, 622 (2007).
[10] C.-Y. Wen *et al.*, Science **326**, 1247 (2009).
[11] N. Geyer *et al.*, Nano Lett. **9**, 3106 (2009).
[12] M. Bruno, M. Palummo, R. Del Sole, V. Olevano, A. N. Kholod, and S. Ossicini, Phys. Rev. B **72**, 153310 (2005).
[13] S. P. Beckman, J. Han, and J. R. Chelikowsky, Phys. Rev. B **74**, 165314 (2006).
[14] X. Zhao, C. M. Wei, L. Yang, and M. Y. Chou, Phys. Rev. Lett. **92**, 236805 (2004).
[15] R. N. Musin and X. Q. Wang, Phys. Rev. B **74**, 165308 (2006).
[16] M. Bruno *et al.*, Phys. Rev. Lett. **98**, 036807 (2007).
[17] M. Bruno, M. Palummo, S. Ossicini, and R. Del Sole, Surf. Sci. **601**, 2707 (2007).
[18] N. Akman, E. Durgun, S. Cahangirov, and S. Ciraci, Phys. Rev. B **76**, 245427 (2007).
[19] J. A. Yan, L. Yang, and M. Y. Chou, Phys. Rev. B **76**, 115319 (2007).
[20] L. Yang, R. N. Musin, X. Q. Wang, and M. Y. Chou, Phys. Rev. B **77**, 195325 (2008).
[21] K. Hong *et al.*, Nano Lett. **8**, 1335 (2008).
[22] D. Yao *et al.*, Nano Lett. **8**, 4557 (2008).
[23] M. Palummo, F. Iori, R. Del Sole, and S. Ossicini Phys. Rev. B **81**, 121303(R) (2010).
[24] J. Xiang *et al.*, Nat. Nanotechnol. **1**, 208 (2006).
[25] M. Amato, M. Palummo, and S. Ossicini, Phys. Rev. B **79**, 201302(R) (2009).
[26] M. Amato, M. Palummo, and S. Ossicini, Phys. Rev. B **80**, 235333 (2009).
[27] In the present work we decided to uniform our NWs diameters definition to the biggest part of the existing literature (see for instance Ref. 5). Then the nanowires indicated here with $d=0.7$, 1.1, 1.5, and 1.9 nm correspond to the NWs with $d=0.4$, 0.8, 1.2, and 1.6 nm in Refs. 16, 17, 25, and 26.
[28] In the mixed geometry every type of atom is bonded in a tetrahedral geometry with four atoms of the other type. In the abrupt NWs there is a planar Si/Ge interface along the shortest dimension of the transverse cross section of the wire. The core-shell NWs are radial heterostructures made by two coaxial cylinders: the internal one (the *core*) is made up by a type of atom and the external one (the *shell*) is made up of the other type of atom.
[29] G. Onida *et al.*, Rev. Mod. Phys. **74**, 601 (2002), and references therein.
[30] www.yambo-code.org; A. Marini *et al.*, Comput. Phys. Commun. **180**, 1392 (2009).
[31] P. Giannozzi *et al.*, http://www.quantum-espresso.org
[32] For more computational details see Ref. 27.
[33] M. Palummo *et al.* (unpublished).
[34] N. Daldosso and L. Pavesi, Laser Photonics Rev. **3**, 508 (2009).
[35] L. Tsybeskov *et al.*, Appl. Phys. A **95**, 1015 (2009).
[36] L. E. Ramos *et al.*, Phys. Rev. B **72**, 045351 (2005).
[37] D. L. Smith and C. Mailhiot, Rev. Mod. Phys. **62**, 173 (1990), and references therein.